Modulation of intestinal growth and differentiation by photoperiod and dietary treatment during smoltification in Atlantic salmon (*Salmo salar*, L.)

Vilma Duarte[1,2#], Pasqualina Gaetano[1,2#], Anja Striberny[3], David Hazlerigg[3], Even H Jorgensen[3], Juan Fuentes[1] and Marco A Campinho[1,4,5*]

[#]Authors with equal contribution

[1]Centre of Marine Science (CCMAR), University of Algarve, 8005-139 Faro, Portugal.

[2] Department of Biology, Faculty of Marine and Environmental Sciences, Campus de Excelencia Internacional del Mar (CEI MAR), University of Cádiz, Puerto Real, 11519 Cádiz, Spain.

[3]Department of Arctic and Marine Biology UiT – The Arctic University of Norway, 9037 Tromsø, Norway.

[4]Algarve Biomedical Centre - Research Institute (ABC-RI), Universidade do Algarve, 8005-139 Faro, Portugal

[5]Faculdade de Medicina e Ciências Biomédicas, Universidade do Algarve, 8005-139 Faro, Portugal

*Corresponding autor:

Marco António Campinho

Algarve Biomedical Centre - Research Institute (ABCRI), Universidade do Algarve, 8005-139 Faro, Portugal

E-mail: macampinho@ualg.pt

Abstract

Previous to seawater (SW) entry, Atlantic salmon undergo smoltification, a process that prepares the fish to enter and thrive in SW. Several physiological changes occur during smolting, especially in osmoregulatory tissues, the gill, and the intestine. Here we characterized the effects of two different, commonly used smoltification regimes during the end of the freshwater phase; photoperiod (long day-short day-long day) and or the addition of salt and amino acid supplements in the diet. We focused on intestinal morphology differentiation, i.e., external perimeter, absorptive perimeter, tissue thickness, and villi density, during the freshwater and seawater phases. In addition, we quantified modification in cell proliferation (PCNA positive) and of Na+, K+-ATPase (NKA) and Na+, K+,2Cl- (NKCCs) co-transporters expression and distribution by immunohistochemistry. These analyses show that anterior and posterior intestines have different developmental dynamics during smoltification. In both intestinal regions, photoperiod and dietary treatment increased the absorptive perimeter. In addition, diet and photoperiod treatments differentially stimulated NKA protein expression in the anterior intestine. NKCC apical-basolateral expression in the enterocytes increased after SW entry in the anterior and posterior intestines. In conclusion, our results show that, as smoltification progresses, the anterior intestine responds more readily to experimental conditions than the posterior intestine. Photoperiod, together with dietary treatment, seems to enhance the development of the capacity to tolerate SW.

Keywords (5)

Atlantic salmon; intestinal morphology; diet treatment; photoperiod treatment; smoltification

Introduction

Atlantic salmon (*Salmo salar* L.) is an anadromous fish that begins its lifecycle in freshwater (FW). Upon reaching a critical size (≈ 12 cm), juveniles undergo morphological, physiological, and behavioural changes termed smoltification. As smolts, they migrate to the sea to take advantage of the favourable feeding conditions in the ocean. The changes occurring during smoltification (or smolting) are pre-adaptive for seawater (SW) migration and marine residency

and have been the target of numerous studies and several excellent reviews (Hoar 1976, McCormick and Saunders 1987, Hoar 1988, McCormick 2012).

In wild fish, seasonal changes in photoperiod (day length) underpin the onset (winter) and completion (spring) of salmon smoltification (McCormick, Shrimpton et al. 2007, McCormick 2012). Hence a compressed summer-winter-summer photoperiodic regime has been used by the salmon farming industry to achieve SW ready smolts before transfer to SW (Duncan and Bromage 1998, Handeland, Björnsson et al. 2003). However, other studies showed that diets supplemented with ion/salt mixtures might stimulate hypo-osmoregulatory ability and hence, seawater tolerance of salmonids (Salman and Eddy 1987, Salman and Eddy 1988, Salman 2009). Therefore, a dietary treatment concept in which pre-smolts are maintained on continuous light (24L:0D; LL) throughout the FW phase and given a salt/ion mixture supplemented feed during the last weeks before SW transfer has been implemented in the farming industry. Despite the common use of such feeds in the smolts production industry, little is known about the physiological responses.

Freshwater juvenile salmon undergoing smoltification develop hypo-osmoregulatory ability by major developmental changes in the osmoregulatory organs, the gill, kidney, and intestine (McCormick and Saunders 1987, Hoar 1988, Evans, Piermarini et al. 2005, Sundell and Sundh 2012, Nisembaum, Martin et al. 2021). Ion- and osmoregulatory homeostasis in FW are sustained by the uptake of Na+ and Cl-, generally by the gills, and by the production of high quantities of dilute urine (Marshall 2002, Grosell 2011, Edwards and Marshall 2012). In gills, Na+ K+ -ATPase (NKA) activity increases during smoltification (Adams, Zaugg et al. 1975, Hoar 1988) and is closely related to salinity tolerance (McCormick, Regish et al. 2009). In SW, this translates physiologically into higher gill secretion of Na+ and Cl- together with reduced urine production (McCormick 2012).

Salmon gill development and physiology during smolting have been extensively studied, but comparatively less is known about the intestine. This is surprising, considering the pivotal role of the intestine in sustaining drinking, nutrient, and fluid absorption essential in the SW environment (Fuentes and Eddy 1997, Grosell 2011, Carvalho, Gregório et al. 2012, Gregório, Carvalho et al. 2013, Gregório, Carvalho et al. 2014, Sundh, Nilsen et al. 2014).

Still, in FW, fish drink minute amounts of water and the uptake of Na+ and Cl- from food in the gastrointestinal tract compensates for the trend in osmotic water gain and passive loss of ions (Grosell 2011). In SW, salmon actively drink water (Fuentes and Eddy 1997) and intestinal water absorption is enabled by NaCl absorption via apical Na+ K+ 2Cl- co-transporter (namely NKCC2) linked to NKA function (Musch, Orellana et al. 1982). In addition, alkalinization of the intestinal fluid allows precipitation of Mg2+, Ca2+, and sulfates, which are excreted with the faeces, thus reducing intestinal fluid osmolality, and enabling water absorption by the intestine (Loretz 1995, Grosell 2011, Edwards and Marshall 2012, Sundell and Sundh 2012).

Given its digestive function, the gastrointestinal tract becomes a very harsh cellular environment that requires constant cell renewal. This leads to increased cell turnover, which enables intestinal capacity to overcome the different conditions and/or environments to which is exposed (Sundell, Jutfelt et al. 2003, Grosell 2011, Dezfuli, Giari et al. 2012, Sundell and Sundh 2012, Sundh, Nilsen et al. 2014, Campinho 2019). Nonetheless, in wild Atlantic salmon SW-adapted post-smolts, the intestine presents differences in morphology along its anterior to posterior length. It passes from a simple anterior tube with single villi to a complex tube with a high number of villi in the posterior intestine (Lokka, Austbo et al. 2013). Therefore, this organization leads to an extended absorption area in the posterior intestine, suggesting that different intestinal regions might be involved in different functions. Despite these differences, both anterior and posterior regions present significant cell proliferation, thus pointing to the high cell turnover rate observed in vertebrate intestines (Lokka, Austbo et al. 2013).

The aim of the present study was two-fold: Firstly, to provide more information about adaptive changes in the intestine during photoperiodic stimulated (control) smoltification and its impact after SW transfer. Secondly, we aimed at comparing the intestinal responses to control smoltification with those arising in the intestine of dietary stimulated salmon pre-smolts. To achieve these aims, morphometrics and cell proliferation changes in the intestine of photoperiodic and dietary treated salmon pre-smolt were compared separately and in combination. We further asked how these experimental regimes affected intestinal ion physiology by analyzing the protein expression and the distribution

of two crucial ion transporters, the Na+/K+ -ATPase (NKA) and the Na+/K+/2Cl- cotransporter (NKCC), fundamental for intestinal function in SW.

2. Material and Methods

2.1. Animals and experimental design

This work is part of a more extensive study (Striberny, Lauritzen et al. 2021) and the experimental design is schematically presented in Fig. 1. The study followed a 2x2 factorial design: factor 1 is photoperiodic treatment in the earlier phase, and factor 2 is diet treatment in the later phase.

Fertilized Atlantic salmon eggs (*Salmo salar* L.) were obtained (AquaGen, Trondheim, Norway) and hatched at the Aquaculture Research Station in Tromsø (Norway), where the experiments were carried out. In March 2017, at start-feeding, juveniles were kept in FW at 4°C till two weeks before the start of the experiment (6th February 2018). During the two weeks, the temperature was increased from 0.5°C/day to 10°C. At the beginning of the experiment (FW1), a body mass mean of ~40g. Until this point, the animals were kept under continuous light (24L:0D).

On 6th February 2018 (FW1), 1400 fish were divided into four circular tanks (300 L/tank) and kept in FW at 10°C. Two tanks were subjected to 6 weeks of short photoperiod treatment with 7h of light and 17h of darkness (7L:17D, SP-LL groups), and the other two groups were kept under 24h of light (24L:0D, LL-LL groups). During this period, all fish were fed a control feed produced specifically for this experiment (see Table 1 for diet composition) only during the 7h of the day with daylight in the SP group. At the end of the 6 weeks at short photoperiod for SP treated (SP-LL) groups (Mar; FW2), the SP treatment groups were brought back to continuous light (24L:0D). At this point, and for the final 6 weeks in FW, the water temperature was increased and maintained at 12°C. During this period, 2 tanks from each photoperiod treatment (LL-LL and SP-LL) were fed with control feed supplemented with salt and the amino acid tryptophan (LL-LL+ diet and SP-LL+ diet groups) while the other two were fed the control feed (Table 1). The experiment comprised 4 treatment groups; two groups fed the control feed and were exposed to two light regimes, SP-LL and

LL-LL, and two dietary treated groups were exposed to the same two light regimes.

At the end of the FW phase (May; FW3), 50 fish from each treatment were transferred to two circular, 300 L tanks supplied with 33‰ SW at 8°C and kept in SW for 2 months. During the SW period, 3 samplings were carried out 1 day in SW (May; SW1), after 7 days in SW (May; SW7), and at the end of the experiment after 60 days in SW (Jul; SW60).

2.2. Sampling and sample collection

Animals of each experimental group were anaesthetized with an overdose of Benzocaine (160ppm; Sigma-Aldrich). Body mass and fork length were measured, blood was collected, and fish were sacrificed by decapitation. The intestine was isolated, and samples of the anterior intestine (caudal of the pyloric caeca till the first sphincter) and posterior intestine (from the pyloric sphincter to the anal sphincter) were collected. Anterior intestine samples for histology were dissected in the first 3 cm caudal to the point of insertion of the last pyloric caeca, whereas posterior intestine samples were dissected from the first 3 cm caudal to the ileocecal valve and before the anal sphincter. Samples from 5 animals in each treatment and sampling time were washed in 1xPBS to remove non-intestinal debris and fixed in 4% PFA/1xPBS overnight at 4°C, washed in PBS, and stored in 100% methanol at -20°C until use.

2.3. Histology, microscopy image acquisition, and morphometric measurements

After processing, anterior and posterior intestine samples were randomly chosen for histological analysis (n=5/intestinal region). These were dehydrated through a graded series of ethanol (70%→100%), and xylene and intestinal regions from 5 different individual fish were embedded in paraffin using a tissue processor (Leica TP1020, Leica). Serial sagittal sections (8 µm) were prepared in a rotary micrometer (Leica) and mounted on glass slides coated with 3-aminopropyltriethoxysilane (APES; Sigma–Aldrich). That allows those tissues from different individuals to be processed simultaneously in the same slide.

Standard Haematoxylin-Eosin staining was performed on dewaxed and rehydrated sections. Briefly, tissues were immersed in Harris Haematoxylin

solution for 30 s, washed in tap water, and distilled water. Afterwards, immersed in Eosin solution for 30 s, washed in distilled water with a few drops of acetic acid, and excess stain washed in tap water. Stained sections were dehydrated and mounted in DPX (Sigma–Aldrich) and allowed to dry overnight at room temperature. Microscopy imaging was carried out using a Leica DM2000 microscope coupled to a Leica DFC 480 digital camera.

When necessary, different images of the same tissue were taken to capture the whole tissue and later stitched in FIJI (Schindelin, Arganda-Carreras et al. 2012) using the stitching plug-in (Preibisch, Saalfeld et al. 2009). Afterwards, the FIJI free-hand drawing tool measured the external perimeter (Pext), the inner surface of the intestine perimeter (from hereafter, the inner surface of the intestine, Pabs), and the wall thickness from the base of the folds to the serosa. Each group's mean total length (TLmean) was used for normalization since it was impossible to measure the individual fish intestine's size during sampling. As well, given that fixation of the tissues was not done individually but in a group manner, TL is the best approach for normalization of this measurement. Therefore, the external perimeter is presented as Pext/TLmean.

The total *villi* number was measured in a single histological slice from a single individual fish. The external perimeter of the corresponding fish was used for normalization. Final intestinal wall thickness, from the crypt base to the serosa layer (supplementary figure 1A), is presented as an average of four measurements taken 90 degrees from each other (n=5/group) and normalized to the external perimeter of the corresponding fish.

2.4. Fluorescent Immunohistochemistry

Sagittal sections of the anterior and posterior intestine (8µm) were processed as described above and rehydrated through a graded crescent series of ethanol:PBS.

Proliferating cell nuclear antigen (PCNA) staining was carried out with a monoclonal mouse anti-PCNA antibody (1:1400; No. M0879; Dako, Glostrup, Denmark). Sections were pre-incubated in 1xTBS/1%BSA for 1 hour, and after the primary antibody was added and incubated overnight at 4°C. After several washes in PBS/0.05% Tween-20, tissues were incubated overnight at 4°C in PBS/10% sheep serum/0.5% Triton-X with secondary antibody Goat Anti-

mouse IgG (H+L)-CF488A (1:600; No. SAB4600043, Merck KGaA, Darmstadt, Germany). Sections were washed in PBS/0.5% Triton-X and mounted with Vectashield® Mounting Medium with DAPI (Vector Lab). Sections were sealed with colourless nail polish.

Detection of alpha-subunit of all Na+, K+ -ATPase isoforms (NKA) was carried out with α5 antibody (1:500; Developmental Studies Hybridoma Bank (DSHB), University of Iowa, Department of Biological Sciences, Iowa City, IA) accordingly to Lebovitz et al. (Lebovitz, Takeyasu et al. 1989). Sections were pre-incubated for two hours in PBS/5% sheep serum/0.2% Triton-X followed by overnight (o/n) incubation with mAB α5 at 4°C in PBS/5% sheep serum/0.2% Triton-X. Afterwards, slides were washed several times in PBS/0.5% Triton-X. The detection was carried out with secondary antibody Goat Anti-mouse IgG (H+L) CF488A (dilution 1:600; No. SAB4600043, Merck KGaA Darmstadt, Germany) mounted with Vectashield® Mounting Medium with DAPI and sealed with colourless nail polish.

Staining of Na+, K+, 2Cl- cotransporters (NKCC1 and 2) was performed with mAbT4 anti-serum (1:20, DSHB, University of Iowa, Department of Biological Sciences, Iowa City, IA; (Lytle, Xu et al. 1995)). Tissues were pre-incubated in PBS /10% sheep serum/0.5% Triton-X for 90 minutes and incubated o/n at 4°C with mAb T4 in pre-incubation solution. Sections were washed with PBS/0.05% Tween-20 and incubated overnight at 4°C with secondary antibody Goat Anti-mouse IgG (H+L) CF488A (dilution 1:600; No. SAB4600043, Merck KGaA, Darmstadt, Germany) in PBS /10% sheep serum/0.5% Triton-X. After washing with PBS/0.5% Triton-X sections were mounted with Vectashield® Mounting Medium with DAPI and sealed with nail polish.

Z-stacks of 5mm were taken using a Zeiss Z2 fluorescent wide-field microscope coupled to a Zeiss HR digital camera using a 405nm and 488nm filter set. Imaging acquisition conditions were kept constant for all tissues.

2.5. Cell counting and fluorescent intensity analysis

The different channels of acquired multichannel z-stacks were separated in FIJI, and a single villus was retrieved for posterior analysis in Ilastik (Berg, Kutra et al. 2019). All images selected were trimmed to have the same area to permit comparisons and processing by Ilastik. To determine cell numbers, images

(DAPI and PCNA) were segmented using Ilastik. To this end, pixel classification was carried out, followed by object classification. A randomly chosen image was used for initial pixel classification, and object classification and established parameters were used for batch segmentation of the remaining dataset. Ilastik segmented images were imported to Fiji, and BoneJ particle analyzer plug-in (Doube 2020) was used to count the total number of nuclei or PCNA positive cells. The percentage of PCNA-positive cells over total nuclei (DAPI) was calculated. A single section per fish was used for this analysis.

Determination of expression levels of NKA and NKCC in the different tissues of the same slide was carried out using Ilastik. NKA or NKCC channel acquired was imported to Ilastik, and pixel classification was followed by object classification. The total pixel intensity was extracted from Ilastik. NKA and NKCC total intensity data were normalized using the total number of nuclei present in the villi analyzed. A randomly chosen image was used for initial pixel classification, and object classification and established parameters were used for batch total intensity measurements of the remainder dataset. Pixel classification images from Ilastik were imported into FIJI and merged with the DAPI channel, and NKA and NKCC channel signals transform using the lookup table fire display to highlight signal intensity differences.

Enterocyte NKCC expression was classified as apical, apical-basolateral, or basolateral accordingly to their distribution relative to DAPI stained nuclei after the maximum projection of z-stacks and manual classification.

2.6. Statistical analysis

For each time point (except FW1), differences in normalized morphometric measurements, proliferation, and NKA and NKCC intensity/expression analysis were established by two-way ANOVA, considering light (LL-LL and SP-LL) and feed (control and dietary treatment) as factors. To evaluate statistical differences over time within each treatment, we used one-way ANOVA, followed by Bonferroni *post-hoc* test. The Bonferroni post-hoc test determined further differences. Differences between light treatments in FW2 in the same intestinal region and differences between anterior and posterior intestine in the same experimental group were carried out using an unpaired t-student test.

Statistical differences in NKCC enterocyte distribution between apical, basolateral, and apical-basolateral were determined by chi-square on trends test.

Statistical differences were considered significant when the p value<0.05. Statistical analyses were carried out using Prism 9.0.0 for macOS (GraphPad software, San Diego, CA, www.graphpad.com).

3. Results

3.1 Histological morphometric measurements

3.1.1. Anterior intestine

At each time point, the intestine's external perimeter (Pext/TLmean) maintains the same dimensions irrespective of experimental treatments (Fig. 2A, Fig. S1). At the end of the FW period (FW3), fish that were subject to light treatment (two-way ANOVA, p=0.0207) presented a significant effect on the external perimeter, but the statistical analysis failed to identify specific differences between groups (Bonferroni, p≥0.05). After 60 days in SW, it was found an interaction of light and diet (two-way ANOVA, p=0.0328) on the anterior intestine Pext/TLmean, but no pairwise differences were identified (Fig. 2A, Bonferroni, p≥0.05). Nonetheless, LL-LL C presented a higher external perimeter regarding the LL-LL diet, although not significantly different (Bonferroni, p=0.08). There were few differences in comparison to the remaining groups (Bonferroni, p>0.55). In all groups after 60 days in SW, the anterior intestines show a higher perimeter than at the beginning of the experiment (Fig. 2A, FigS1, one-way ANOVA, p<0.001, Supplementary Table 1). The data argue that there are no overall differences in intestinal growth between experimental conditions.

To understand if there was an increase in the intestinal interface responsible for ion exchange, we measured the absorptive perimeter (inner perimeter of the anterior intestine) and normalized it to the external perimeter of the respective tissue (Pabs/Pext). From the beginning of the experiment until SW60, all groups presented an increase in Pabs/Pext (one-way ANOVA, Bonferroni, p<0.001, Supplementary Table 2), except SP-LL+diet, which remained constant (Bonferroni, p>0.05, table 2, supplementary data). The exposure of pre-smolts

to a short-day light regime (FW2) decreased the anterior intestine Pabs/Pext compared to fish in continuous light (Fig. 2B, Fig.S1; unpaired t-test, $p=0.0090$). However, at the end of the FW period (FW3), no differences were found between experimental groups Pabs/Pext (Fig. 2B, Fig. S1, two-way ANOVA, $p\geq0.05$). Despite this, just after 1 day in, SW fish that had been exposed to continuous light and receiving dietary treatment (Fig. 2B LL-LL+diet, Fig. S1) had higher Pabs/Pext than short-day exposed animals (two-way ANOVA, light, $p=0.0007$, Bonferonni, $p<0.05$). No differences in Pabs/Pext were found between fish maintained at constant light and fed with either diet (Fig. 2B, Fig. S1, 2-way ANOVA, light, $p=0.0007$, Bonferonni, $p>0.05$). The differences found in Pabs/Pext at 1 day in SW were lost after 7 days even though there was a significant effect of light (Fig. 2B, Fig. S1, two-way ANOVA, light, $p=0.0007$, Bonferonni, $p>0.05$). At the end of the experiment (SW60), these groups showed a significant interaction between light and dietary treatment (Fig. 2B, Fig. S1, two-way ANOVA, $p=0.0283$). However, a pairwise comparison of Pabs/Pext between SW60 groups showed that only LL-LL C and LL-LL+diet were different (Fig. 2B, Fig. S1, Bonferonni, $p<0.05$).

The anterior intestine total number of *villi* per section analyzed was determined and normalized to the individual fish's external perimeter (Pext) (*villi*/Pext, Fig. 2C). Pre-smolts exposed to short days (SP-LL) presented a lower ratio of *villi*/ Pext in comparison to continuous light fish (LL-LL) (Fig. 2C, FW2; t-test, $p=0.009$). By the end of the FW period and after different dietary treatments (FW3), there were no differences found between treatments (Fig. 2C, two-way ANOVA, $p>0.05$). These observations were maintained in the fish after 1 and 7 days in SW (Fig. 2C, two-way ANOVA). Although in SW1, there was a significant variation of *villi*/Pext ratio with a significant interaction between light and diet (Fig. 2C, two-way ANOVA, interaction $p=0.03$) these differences did not present any pairwise differences (Bonferroni, $p>0.05$). While there was a slightly positive overall effect of salt diet on the ratio *villi*/ Pext ($p=0.0088$), this effect was highly dependent on prior photoperiodic treatment. In LL fish, salt increased *villi* number by ~50% (Fig. 2C, Bonferroni, $p=0.0037$), whereas in SP treated fish, there was no significant dietary effect (Fig. 2C, Bonferroni, $p>0.05$). At the end of the experiment (SW60), LL-LL C, SP-LL C, and SP-LL+diet

371 groups suffer a decrease in the ratio of *villi*/Pext in relation to the previous
372 sampling (SW7) (Fig. 2C; Supplementary Table 3, one-way ANOVA, $p<0.05$).
373 Wall thickness of the anterior intestine was determined and normalized by the
374 external perimeter of individual fish (thickness/Pext, Fig. 2D). There was a
375 significant decrease in thickness/Pext from FW1 to SW60 in all treatment
376 groups (Fig. 2D, one-way ANOVA, $p<0.001$, supplementary table 4). In FW 3,
377 there is a general effect of photoperiod on thickness/Pext, but the statistical
378 analysis does not show specific differences between groups (Fig. 2D; two-way
379 ANOVA, $p>0.05$).
380
381 **3.1.2. Posterior intestine**
382 A similar morphometric analysis was carried out in the posterior intestine (Figs.
383 2E-H) after hematoxylin-eosin staining (Fig. S2).
384 From the start of the experiment (FW1) to SW60, there was a significant
385 increase in the size (Pext/TLmean) of the posterior intestine in all experimental
386 groups (Fig. 2E; Supplementary Table 5, one-way ANOVA, $p<0.01$). In FW, no
387 differences were found between experimental groups (Fig. 2E, two-way
388 ANOVA, $p>0.05$). However, at SW7 and SW60, we detected a significant
389 interaction between light and dietary treatment (Fig. 2E, two-way ANOVA,
390 interaction $p<0.05$), although no pairwise differences were found between
391 experimental groups.
392 The posterior intestine absorptive perimeter (Pabs/Pext) significantly increased
393 in LL-LL C, LL-LL+diet, and SP-LL C groups (Fig. 2F, one-way ANOVA
394 $p<0.002$, supplementary table 6). However, pairwise comparisons showed no
395 differences in Pabs/Pext between SW60 and FW1 in the LL-LL C and SP-
396 LL+diet groups (Fig. 2, Bonferroni, $p>0.05$). Significant differences between
397 treatments were only detected at SW7 and between LL-LL+diet and the SP
398 groups (Fig. 2F, Bonferroni, $p<0.05$).
399 The ratio *villi*/Pext increased slightly but significantly from FW1 to SW60 in all
400 experimental groups (Fig. 2G; Supplementary Table 7, one-way ANOVA,
401 $p<0.05$), although no pairwise differences were found (Bonferroni, $p>0.05$).
402 Also, no pairwise differences were found between experimental groups at each
403 time point (Fig. 2G, Bonferroni, $p>0.05$). However, a significant interaction
404 between light and diet was observed in SW1 (two-way ANOVA, $p=0.0167$) and

SW7, with a significant effect of dietary treatment (two-way ANOVA, p=0.0276; Fig. 2G)

Posterior intestine wall thickness (thickness/Pext) did not change in the LL-LL C group from FW1 to SW60 (Fig. 2H, one-way ANOVA, $p>0.05$), but it was significantly lower in the remaining groups (one-way ANOVA, $p<0.05$; supplementary table 8). In all experimental time points, there were no significant differences in thickness/Pext between groups (Fig. 2H, two-way ANOVA, $p>0.05$).

3.2 Anterior versus posterior intestine

The posterior intestine was wider and presented a higher absorptive surface than the anterior intestine during all time points and in most experimental groups (Fig. 2, t-test, $p<0.05$, supplementary tables 9 and 10). Except for SW60, no differences were found in Pext/TLmean between LL-LL C anterior and posterior intestine (Fig. 2, t-test, $p>0.05$, supplementary table 9). In contrast, no differences were found in *villi*/Pext between the two intestinal regions (Fig. 2C and 2G, t-test, $p<0.05$, supplementary table 11). The only exception was found in SW7 SP-LL+diet and SW60 SP-LL C, where the posterior intestine had a higher number of *villi* (Fig. 2C and 2G, t-test, $p\leq0.0088$, supplementary table 11). Intestinal wall thickness (thickness/Pext) was higher in the anterior intestine than in the posterior intestine in most groups at the different time points (Fig. 2D and 2F, t-test, $p<0.05$, supplementary table 12). No differences in thickness/Pext were found between anterior and posterior intestines of FW3 LL-LL C, SW60 LL-LL C, and SW60 SP-LL C groups (Fig. 2D and 2F, t-test, $p>0.05$, supplementary table 12).

3.3. Intestinal Cell proliferation

Given the high cellular turnover rate of the intestine and the known effect of light and feeding regimes on intestinal cell proliferation (Peyric, Moore et al. 2013), the effect of the different treatments on cell proliferation during the experiment in the anterior intestine was also investigated (Fig. 3A, Fig. S3). Proliferative cells, as determined by PCNA staining, were primarily found at *villi* crypts located in the intestine's proximal region (anterior intestine) (Fig. S2). Quantitative assessment of cell proliferation (%PCNA) in the intestine was

carried out in single *villi*/individual and showed no significant changes between FW1 and SW60 (Fig. 3A; one-way ANOVA, $p>0.05$; supplementary table 13). However, at FW3, LL-LL+diet presented higher cell proliferation when compared to SP-LL+diet (Fig. 3A, two-way ANOVA, Bonferroni, $p<0.0001$) and LL-LL C (Bonferroni, $p=0.0084$) groups. In SW1, light significantly affects cell proliferation (Fig. 3A, two-way ANOVA, light $p=0.0069$, interact). At the end of the experiment (SW60), cell proliferation was similar to those observed in FW3 (Fig. 3A). An effect of light and interaction between light and dietary treatment was observed (two-way ANOVA, $p=0.0267$ and $p=0.0019$, respectively). In this last time point, the LL-LL+ diet and SP-LL+ diet groups were significantly different (Bonferroni, $p=0.0013$), but no other differences were found (Fig. 3A, Bonferroni, $p>0.05$).

The presence of proliferative cells in the posterior intestine was observed on *villi* crypts and the most proximal lateral side of the *villi* (Fig. S4). Quantification of posterior intestine cell proliferation revealed variation during the time course of the experiment in all experimental groups (Fig. 3B, one-way ANOVA, $p<0.05$, supplementary table 14). However, a significant decrease in proliferation was only found in LL-LL groups at SW60 vs FW1 (Fig. 3B, Bonferroni, $p<0.001$; supplementary table 14). There were no differences between groups at FW2 (Fig. 3B, t-test $p>0.05$), but at FW3, SP-LL C had lower cell proliferation than the LL-LL groups (Fig. 3B, Bonferroni, $p<0.05$). Just after 1 day in SW, both dietary treatments and the combination of light and diet showed a significant response to cell proliferation (Fig. 3B; two-way ANOVA, $p=0.033$, and $p=0.0012$, respectively). In SW1, the LL-LL+diet group had lower cell proliferation than the LL-LL C group (Fig. 3B, Bonferroni, $p<0.0015$), but no other differences were found. After 7 days in SW, there were no differences within LL-LL groups, but these presented differences in the SP groups (Fig. 3B, Bonferroni, $p<0.05$). In SP groups, the absence or presence of the dietary treatment had the opposite effect on cell proliferation, with the SP-LL C group presenting the highest and the SP-LL+diet groups having the lowest proliferation rate (Fig. 3B, Bonferroni, $p<0.05$).

Differences in cell proliferation between anterior and posterior intestines were highly variable accordingly to experimental time points and groups (Fig 3A and 3B; supplementary table 15). Overall, anterior intestine cell proliferation is more

constant, whereas the posterior intestine presents higher variability (Fig. 3A and 3B), and in general, the posterior intestine presented a higher percentage of proliferation than the anterior intestine (supplementary table 15).

3.4. NKA and NKCC distribution

3.4.1 Na+ K+ - ATPase pump

NKA is expressed in anterior and posterior intestine enterocytes at all-time points, and experimental groups were analyzed (Fig. 4, S5, and S6). The intensity of the Na+ K+ - ATPase pump was measured in both regions of the intestine using a quantitative workflow and represented as pixel total intensity (Figure 4).

During the experiment, anterior intestine, NKA expression only varied significantly in the LL-LL+ diet group (Fig. 4A, S5; supplementary table 16, one-way ANOVA, $p=0.0004$). However, pairwise comparisons only found significant NKA expression increase in FW1vsSW1 (Bonferroni, $p<0.05$), FW2vsSW1 (Bonferroni, $p<0.001$), FW3vsSW1 (Bonferroni, $p<0.0001$) and significant decrease in SW1vsSW60 (Bonferroni, $p<0.001$; supplementary table 16). Dietary treatment significantly affected NKA expression at FW3 (Fig. 4A, S5; two-way ANOVA, $p=0.0036$). In the LL-LL+ diet group, NKA expression was significantly lower than in SP-LL C (Bonferroni, $p<0.05$) but not compared to the other groups (Fig. 4A, S5; Bonferroni, $p>0.05$). After 1 day in SW, light treatment (Fig. 4A, S5; two-way ANOVA, $p=0.0083$) had a significant statistical effect on the increased NKA expression. Still, in SW1 in the LL-LL+ diet group, NKA expression was higher than in SP groups (Bonferroni, $p<0.05$), but no significant differences were found in LL-LL C (Fig. 4A, S5; Bonferroni, $p>0.05$). In both SW7 and SW60, no pairwise differences were found between experimental groups (Fig. 4A, S5; Bonferroni, $p>0.05$). In SW60, the NKA expression showed a significant interaction between light and dietary treatment ($p=0.0289$).

In the posterior intestine, there were no significant differences in NKA expression between experimental groups within any time point (Fig. 4B, S6;

two-way ANOVA, p>0.05) nor for the duration of the experiment (one-way ANOVA, p>0.05; supplementary table 17).

In most time points and experimental groups, average NKA expression was similar between the anterior and posterior intestine (Fig. 4, S5 and S6; t-test, p>0.05, supplementary table 18). NKA expression was higher in the posterior intestine at FW2 LL-LL (t-test, p=0.0067), FW3, and SW60 LL-LL+diet (t-test, p=0.037) but lower in SW1 LL-LL+diet (Fig. 4, S5 and S6; t-test, p=0.037, supplementary table 18).

3.4.2. NKCC co-transporters

After staining, we used the Ilastik quantitative expression workflow to have a quantitative assessment of NKCC expression in both intestinal regions (Fig. 5A and B; S7 and S8). The quantitative expression results are represented as a function of maximum pixel intensity over the total number of cells (as determined by DAPI, segmentation, and cell count). As expected, the expression of NKCC co-transporters is specific to enterocytes in both the anterior and posterior intestine (Fig. S7 and S8).

In the anterior intestine, expression of NKCC transporters varied significantly during the time course of the experiment in LL-LL C (one-way ANOVA, p<0.0001), SP-LL C (one-way ANOVA, p<0.0493), and SP-LL+diet (one-way ANOVA, p<0.0001) groups but not in LL-LL+diet (one-way ANOVA, p>0.05, supplementary table 19). Significant differences between time points in each experimental condition were only found in LL-LL C and SP-LL+diet from FW2 and FW3 to SW7 and in the LL-LL C group from SW1 to SW7, there was a significant increase in NKCC (Bonferroni, p<0.0001, supplementary table 19). However, at SW60 in both experimental groups, NKCC expression decreased compared to SW7 to FW levels (Fig. 5A; Bonferroni, p<0.01, Supplementary Table 19).

A pairwise comparison of NKCC expression in FW2 revealed that exposure to short days decreased the expression of NKCC cotransporter proteins in the SP group (Fig. 5A, S7; Bonferroni, p<0.05). At FW3, no differences were found between experimental groups (Fig. 5A, Bonferroni, p>0.05) even though there was a significant effect due to interaction between light and diet at this time point (two-way ANOVA, interaction p=0.0341). Just after 1 day in SW, there

was a significant effect of light on NKCC expression (two-way ANOVA, p=0.006), but pairwise comparison revealed that only LL-LL C and SP-LL+diet groups were significantly different with higher expression in the latter (Fig. 5A; Bonferroni, p<0.05). In SW7, all groups had similar expressions of NKCC. This relation was maintained in SW60 (Fig. 5A, two-way ANOVA, p>0.05).

In the posterior intestine, NKCC expression significantly varied in LL-LL C, LL-LL+diet, and SP-LL+diet groups (one-way ANOVA, p<0.05; Supplementary Table 20) but not in SP-LL C (Fig. 5B, S8; one-way ANOVA, p>0.05). Nonetheless, no differences in NKCC expression were found between FW1 and SW60 in any experimental group (Fig. 5B; Bonferroni, p>0.05, supplementary table 20).

Within time points, there were no significant differences in NKCC expression at FW2, despite large differences in averages (Fig. 5B, t-test, p<0.05). That is likely due to the low number of replicates in the SP group (n=2). By FW3, all experimental factors and the interactions between them contributed to the observed variation in the expression of NKCC (Fig. 5B; 2-way ANOVA, p<0.05). Pairwise comparisons revealed that at FW3, the LL-LL C group showed a higher expression in relation to all other groups (Fig. 5B, S8; Bonferroni, p<0.05), but no differences were found between the other groups (Bonferroni, p>0.05). After 1 day in SW, no differences were found between groups (Fig. 5B, one-way ANOVA, p>0.05). However, at SW7, light and dietary treatment, but not their interaction, had significant effects on NKCC expression (Fig. 5B, S8; Two-way ANOVA, p<0.05), and pairwise comparisons confirmed that the LL-LL+diet group had a higher expression than any other group (Bonferroni, p<0.05). By SW60, no differences were found in NKCC expression (Fig. 5B, two-way ANOVA, p>0.05).

In parr (FW1), the anterior intestine had higher expression of NKCC than the posterior intestine (Figs. 5A and B, S7 and S8; t-test, p=0.0296, supplementary table 21). This difference was maintained in FW2 LL-LL (t-test, p=0.0002, supplementary table 21) but not in the SP group (t-test, p>0.05, supplementary table 21). In FW3, only the anterior intestine of SP-LL C groups presented higher expression of NKCC than the posterior (Figs. 5A and 5B, S7 and S8; t-test, p=0.0475). That continued in SW1 (t-test, p=0.0169) and SW7 (t-test, p=0.0004). In SW1 and SW7, NKCC expression in the SP-LL+diet group was

higher in the anterior intestine (Figs. 5A and 5B, S7 and S8; t-test, p<=0.0084). At SW7, there was also a significantly higher anterior intestine expression of NKCC in the LL-LL C group (Figs. 5A and 5B, S7 and 8; t-test, p<0.0001; supplementary table 21). No differences between the anterior and posterior intestine expression of NKCC were found at SW60 (Figs. 5A and 5B, S7 and S8; t-test, p>0.05, supplementary table 21).

mT4 anti-serum labels both NKCC1 and NKCC2; the former is basolateral and the latter apical (Lytle, Xu et al. 1995). Therefore, we used this to further characterize their protein distribution in the intestine. To address NKCC1 and NKCC2 contributions to expression results, *villi* enterocytes in the anterior and posterior intestine were counted, and NKCC signal distribution (as a percentage of total enterocytes identified by DAPI) was determined (Fig. 5C and D; S7 and S8) as apical (NKCC2) basolateral (NKCC1) or apical/basolateral (NKCC1+NKCC2). In the anterior intestine at FW1, there is an equivalent distribution of basal and apical/basolateral and basolateral NKCC expression, with <10% of enterocytes having only apical expression (Fig. 5C and S7). From FW1 to SW60, there is a gradual increase of enterocytes with apical/basolateral signals that, at the end of the experiment, constitute the majority (>90%) of enterocytes in all treatments (Fig. 5C, S7, and S8, chi-square on trends, p<=0.0151, supplementary table 22A). Comparisons between experimental groups at each time point revealed that FW2 light does not affect anterior NKCC signal distribution (chi-square on trends, p>0.05) and that time alone drives this to become more apical/basolateral (Fig. 5C and S7, chi-square on trends, p<0.0001; supplementary table 22B). A higher apical distribution was observed in LL-LL C and SP-LL+diet groups in FW3 (Fig. 5C and S7; chi-square on trends, p<0.05; supplementary table 22B), and at SW1, no differences are found (chi-square on trends, p>0.05, supplementary table 22). Nonetheless, after 7 days in SW, NKCC distribution is only similar between LL-LL+diet and SP-LL C and LL-LL C and SP-LL+diet groups (Fig. 5C and S7; chi-square on trends, p>0.05; supplementary table 22B). At the end of the experiment at SW60, there are only significant differences in NKCC distribution between LL-LL+diet and both SP-LL groups (Fig. 5C and S7, chi-square on trends, p<0.05, supplementary table 22B).

608 The distribution pattern of NKCC at FW1 in the posterior intestine was similar to
609 the anterior intestine (Figs. 5C and 5D). During the experimental period, there
610 was a significant gradual change in the distribution of NKCC expression to
611 apical/basolateral (>90%) at SW60 (Fig. 5D and S8; chi-square on tends,
612 $p<0.0001$; Supplementary Table 23A). In the posterior intestine of the SP group
613 at FW2, we identified a significant shift in the distribution of NKCC to
614 apical/basolateral (Fig. 5D and S8; chi-square on trends, $p<0.0001$,
615 supplementary table 23B). Light and, to some extent, dietary treatment drive
616 NKCC expression apical/basolateral at FW3 and SW1 (Fig. 5D and S8; chi-
617 square on trends, $p<0.05$, supplementary table 23B). However, at SW7, the diet
618 is more important in driving apical/basolateral expression of NKCC (Fig. 5D and
619 S8; chi-square on trends, $p\leq0.0018$, supplementary table 23B). Notably, SW60
620 light is again more important in establishing posterior intestine apical/basolateral
621 NKCC expression (Fig. 5D and S8; chi-square on trends, $p<0.05$,
622 supplementary table 23B).
623
624 **4. Discussion**
625 The main objective of this work was to characterize the intestinal changes
626 during photoperiodic and dietary treatments during Atlantic salmon
627 smoltification and after SW transfer. Morphology, cell proliferation (PCNA +),
628 and the distribution of the two main ion transporters, NKA and NKCC co-
629 transporters, were analyzed in the anterior and posterior intestines.
630 Functional studies in *Dicentrarchus labrax* revealed that the anterior (and mid-)
631 intestine are likely involved in ingested fluid processing to drive down intestinal
632 fluid osmolality, whereas the posterior intestine is more involved in water
633 absorption (Alves, Gregório et al. 2019). In contrast, in *Sparus aurata*, there
634 does not seem to exist such regional compartmentalization of fluid processing
635 and water absorption (Gregório, Carvalho et al. 2013). Evidence suggests that
636 water absorption rates are higher at the anterior than in the posterior intestine
637 of *S. aurata* (Carvalho, Gregório et al. 2012) and indicate species-specific
638 adaptations. In seawater-adapted Atlantic salmon, the posterior intestine seems
639 to have higher water absorption than the anterior intestine (Veillette, White et al.
640 1993, Sundell, Jutfelt et al. 2003) suggesting that the two intestinal
641 compartments have different functions. Our data reinforce these previous

642 observations on the different functions of the anterior and posterior intestinal
643 regions in Atlantic salmon.
644 Atlantic salmon anterior and posterior intestinal development has different
645 dynamics during the experimental time. The anterior intestine grows faster in
646 diameter and length, while the posterior develops more complex *villi*, resulting in
647 a higher absorptive surface. That is likely a strategy to compensate for the
648 shorter length of the posterior intestine (Caspary 1992, Khojasteh 2012). The
649 increase in *villi* and the absorptive surface is due to increased cell proliferation
650 observed in the posterior intestine. Those observations are in line with previous
651 studies on wild salmon (Lokka, Austbo et al. 2013).
652 At the end of the experimental time (SW60), constant light and diet enhanced
653 absorptive perimeter, number of *villi*, and cell proliferation in the anterior
654 intestine but not in the posterior intestine. That argues that constant light plus
655 diet treatment has the potential to condition anterior intestine reshaping during
656 SW adaptation. In contrast, experimental conditions did not affect the posterior
657 intestine morphological parameters measured even though cell proliferation was
658 enhanced in light-treated fish. This argues that, in FW, the anterior intestine is
659 more responsive to experimental conditions than the posterior intestine.
660 Nonetheless, photoperiodic history has been shown to have a significant impact
661 on intestinal homeostasis in mammals (Stokes, Cooke et al. 2017, Codoñer-
662 Franch and Gombert 2018) and zebrafish (Peyric, Moore et al. 2013). The
663 proliferation of intestinal stem cells is detrimentally affected by changes in
664 photoperiod in drosophila (Parasram, Bernardon et al. 2018, Parasram and
665 Karpowicz 2020) but also in mammals (Brown 2014, Stokes, Cooke et al.
666 2017). For the first time, our data suggest that salmon intestinal cell proliferation
667 during smolting and SW adaptation is responsive to photoperiod history and
668 manipulation.
669 Nonetheless, the finding that in constant light-treated fish (LL-LL C), cell
670 proliferation in the anterior intestine is higher than in short-day treated fish (SP-
671 LL C) also suggests that other factors, besides photoperiodic history, contribute
672 to anterior intestinal cell renewal. On the other hand, the data suggest that a
673 short day might hamper cell proliferation in the anterior intestine. However, the
674 opposite seems to be true for the posterior intestine. Thus, it is possible that,
675 like in zebrafish (Peyric, Moore et al. 2013), regular feeding also plays a role

676 during salmon intestinal smolting development or that factors acting to promote
677 smoltification are responsible for increased intestinal cell proliferation regardless
678 of photoperiodic history.
679 At the end of the experiment (60 days in SW), diet alone (under continuous light
680 conditions) was able to elicit some of the same responses observed on light
681 stimulated fish, e.g., an increase in the absorptive perimeter, number of *villi*, and
682 cell proliferation on intestinal development, especially in the anterior intestine.
683 Our findings in the present study argue that dietary treatment elicits some
684 responses of light enhanced intestinal development that may explain why feed
685 intake and specific growth rate in these fish reflect those of SP-LL treated fish
686 after SW transfer (Striberny, Lauritzen et al. 2021).
687
688 A crucial physiological aspect of Atlantic salmon smoltification is the acquisition
689 of SW tolerance and the ability to hypo-osmoregulate in SW (McCormick 2012).
690 During smolting, a series of physiological changes occur so that the intestine
691 can absorb water after SW entry. An organism-integrated action where the gills
692 undergo the inverse transition, passing from an ion absorption role to a
693 secretory role, especially of the monovalent ions Na+ and Cl-. Besides a
694 change in the catalytic ionocyte composition, gill NKA expression and activity
695 increase during smoltification and hence have long been used as a marker of
696 smoltification progression (Zaugg and McLain 1976). Nonetheless, evidence
697 suggests that gill NKA activity might not always be a good indicator of salinity
698 tolerance in Atlantic salmon smoltification (Åse, Arne et al. 1995, Iversen,
699 Mulugeta et al. 2020). In the salmon intestine enterocytes, NKAa1a, a1b, and
700 a1c are expressed in FW and after SW transfer. Only NKAa1c seems actively
701 regulated during smoltification, where it passes from a basal localization in FW
702 to basolateral localization in SW (Sundh, Nilsen et al. 2014). In the present
703 study, NKA expression dynamically responded to photoperiod and dietary
704 treatment and during time course on the anterior but not in the posterior
705 intestine (Figs. 4A and 4B). At the end of the FW period, the dietary treatment
706 decreased, in comparison to control diet treatments, NKA anterior intestine
707 expression.
708 Nonetheless, as soon as the fish were transferred to SW, only continuous light
709 plus dietary treated fish was able to upregulate NKA expression, suggesting

that dietary treatment on its own, and in the absence of a short-day treatment, can enhance NKA expression after just 1 day in SW (Fig. 4A). However, NKA expression in all groups is already identical after 7 days in SW (Fig. 4A). That argues that dietary treatment enhances the osmoregulatory capacity of the anterior intestine, likely by regulation of NKA expression and other mechanisms not clear from our study (Fig. 4A). Comparison with NKA activity measured in the same experiment reveals that anterior intestine NKA activity is less variable than protein expression (Gaetano, et al, in submission) possibly highlighting the contribution of other factors to NKA activity only than expression. At SW7, the comparison between NKA activity (Gaetano, et al, in submission) and expression are closely correlated.

On the other hand, in the posterior intestine, the activity of NKA was stimulated by the light treatment (Gaetano, et al, in submission) even though the expression was unaltered. Collectively this suggests that during smolting salmon, intestinal NKA activity is not dependent on protein expression alone, but other factors might be necessary. In previous work in *Sparus aurata*, we show that transport and subcellular localization are essential for intestinal osmoregulatory capacity (Gregório, Carvalho et al. 2013). It is also likely to reflect the contribution of different NKA isoforms to activity (Sundh, Nilsen et al. 2014), which we could not be resolved with the anti-NKA anti-serum used.

NKCC transporters are also dynamically regulated during salmon smoltification (Tipsmark, Madsen et al. 2002, Sundh, Nilsen et al. 2014). The longer the fish spend in SW apically located NKCC2 becomes more expressed together with basolateral NKCC1 that is already expressed in FW (Sundh, Nilsen et al. 2014). We have previously demonstrated that in the same fish used in this study, ex vivo apical pharmacologic inhibition of NKCC2 leads to decrease absorptive capacity both in FW and after 7 days in SW, indicating a role for NKCC2 in SW adaptation (Gaetano, et al, in submission). NKCC1 and NKCC2 expression are differentially regulated by light and diet treatments in both the anterior and posterior intestine (Figs. 5A and 5B). Enterocytes only expressing NKCC1 are abundant in pre-smolts (basal located; FW1), but as soon as fish undergo photoperiod manipulation (FW2), there is a significant increase in apical and apical/basal localization of NKCC immunostaining that reveals an increase in

744 NKCC2 expression. That event might signal the first step in the preparedness
745 for smoltification and the subsequent adaptation of salmon to SW transfer.
746 However, a key difference lies in the timing of the response of each intestinal
747 region. In the anterior intestine, NKCC expression is enhanced in short-term
748 SW exposure after short days and dietary treatment. This effect becomes
749 diluted after 7 and/or 60 days in SW (Fig. 5A). The posterior intestine responds
750 differently, and only after 7 days in SW increased expression is apparent in LL-
751 LL+diet groups, but that is lost at SW60 (Fig. 5B). Nonetheless, a crucial
752 observation is that in both intestinal regions, as soon the fish enter SW, the
753 percentage of apical/basolateral expression increases (Figs. 5C and 5D),
754 arguing that SW exposure is the ultimate signal responsible for this intestinal
755 response.
756
757 In conclusion, our data show that anterior and posterior intestines have different
758 developmental dynamics during smoltification and SW adaptation.
759 Our results indicate that as smoltification progresses and size increases, the
760 histological and molecular traits required for the acquisition of SW tolerance
761 develop. Photoperiod and dietary treatment seem to enhance the development
762 of this capacity. Notably, dietary treatment alone increased the anterior intestine
763 absorptive area. The combination of photoperiod and dietary manipulation can
764 be advantageous from an aquaculture perspective.
765
766 **Acknowledgments**
767 We appreciate the support of the staff at Tromsø Aquaculture Station for taking
768 care of the fish and helping with feed intake measurements. We would further
769 like to thank Anja Sjøvoll, Bjørn Ellingsen, and Daniel Lauritzen for practical
770 help during the sampling and archiving of the data. The T4 and a5 developed,
771 respectively, by Yale University and Johns Hopkins University were obtained
772 from Developmental Studies Hybridoma Bank., created by the NICHD of the
773 NIH and maintained at the University of Iowa, Department of Biology, Iowa City,
774 IA 52242. We acknowledge, also, to the Light Microscopy Unit of ABC-RI.
775
776 **Funding**

This project was funded by FHF - Norwegian Seafood Research Fund, Project no. 901432. CCMar receives Portuguese national funds from FCT - Foundation for Science and Technology through projects UIDB/04326/2020, UIDP/04326/2020, and LA/P/0101/2020. The Microscopy Unit was partially supported by national portuguese funding FCT: PPBI-POCI-01-0145-FEDER-022122. Vilma Duarte and Pasqualina Gaetano are currently supported by FCT with Ph.D. grants 2021.04507.BD and SFRH/BD/140045/2018, respectively. MAC was a recipient of an FCT-IF Starting Grant (IF/01274/2014).

Competing interests

On behalf of all authors, the corresponding author states that there is no conflict of interest.

References

Adams, B. L., W. S. Zaugg and L. R. McLain (1975). "Inhibition of salt water survival and Na-K-ATPase elevation in steelhead trout (Salmo gairdneri) by moderate water temperatures." Transactions of the American Fisheries Society **104**(4): 766-769.

Alves, A., S. F. Gregório, R. C. Egger and J. Fuentes (2019). "Molecular and functional regionalization of bicarbonate secretion cascade in the intestine of the European sea bass (Dicentrarchus labrax)." Comparative Biochemistry and Physiology Part A: Molecular & Integrative Physiology **233**: 53-64.

Åse, I. B., B. Arne, B. Trygg, H. Tom, F. Hans Jørgen and O. S. Sigurd (1995). "Development of salinity tolerance in underyearling smolts of Atlantic salmon (Salmo salar) reared under different photoperiods." Canadian Journal of Fisheries and Aquatic Sciences **52**(2): 243-251.

Berg, S., D. Kutra, T. Kroeger, C. N. Straehle, B. X. Kausler, C. Haubold, M. Schiegg, J. Ales, T. Beier, M. Rudy, K. Eren, J. I. Cervantes, B. Xu, F. Beuttenmueller, A. Wolny, C. Zhang, U. Koethe, F. A. Hamprecht and A. Kreshuk (2019). "ilastik: interactive machine learning for (bio)image analysis." Nature Methods **16**(12): 1226-1232.

Brown, S. A. (2014). "Circadian clock-mediated control of stem cell division and differentiation: beyond night and day." Development **141**(16): 3105-3111.

Campinho, M. A. (2019). "Teleost Metamorphosis: The Role of Thyroid Hormone." Front Endocrinol (Lausanne) **10**: 383.

Carvalho, E. S. M., S. F. Gregório, D. M. Power, A. V. M. Canário and J. Fuentes (2012). "Water absorption and bicarbonate secretion in the intestine of the sea bream are regulated by transmembrane and soluble adenylyl cyclase stimulation." Journal of Comparative Physiology B **182**(8): 1069-1080.

Caspary, W. F. (1992). "Physiology and pathophysiology of intestinal absorption." Am J Clin Nutr **55**(1 Suppl): 299s-308s.

Codoñer-Franch, P. and M. Gombert (2018). "Circadian rhythms in the pathogenesis of gastrointestinal diseases." World J Gastroenterol **24**(38): 4297-4303.
Dezfuli, B. S., L. Giari, A. Lui, S. Squerzanti, G. Castaldelli, A. P. Shinn, M. Manera and M. Lorenzoni (2012). "Proliferative cell nuclear antigen (PCNA) expression in the intestine of Salmo trutta trutta naturally infected with an acanthocephalan." Parasites & Vectors **5**(1): 198.
Doube, M. (2020). "Multithreaded two-pass connected components labelling and particle analysis in ImageJ." bioRxiv: 2020.2002.2028.969139.
Duncan, N. J. and N. Bromage (1998). "The effect of different periods of constant short days on smoltification in juvenile Atlantic salmon (Salmo salar)." Aquaculture **168**(1): 369-386.
Edwards, S. L. and W. S. Marshall (2012). 1 - Principles and Patterns of Osmoregulation and Euryhalinity in Fishes. Fish Physiology, edit by S. D. McCormick, A. P. Farrell and C. J. Brauner, Academic Press. **32:** 1-44.
Evans, D. H., P. M. Piermarini and K. P. Choe (2005). "The Multifunctional Fish Gill: Dominant Site of Gas Exchange, Osmoregulation, Acid-Base Regulation, and Excretion of Nitrogenous Waste." Physiological Reviews **85**(1): 97-177.
Fuentes, J. and F. B. Eddy (1997). "Drinking in Atlantic Salmon Presmolts and Smolts in Response to Growth Hormone and Salinity." Comparative Biochemistry and Physiology Part A: Physiology **117**(4): 487-491.
Fuentes, J. and F. B. Eddy (1997). Drinking in marine, euryhaline and freshwater teleost fish. Ionic Regulation in Animals: A Tribute to Professor W.T.W.Potts**:** 135-149.
Gregório, S. F., E. S. M. Carvalho, M. A. Campinho, D. M. Power, A. V. M. Canário and J. Fuentes (2014). "Endocrine regulation of carbonate precipitate formation in marine fish intestine by stanniocalcin and PTHrP." The Journal of Experimental Biology **217**(9): 1555-1562.
Gregório, S. F., E. S. M. Carvalho, S. Encarnação, J. M. Wilson, D. M. Power, A. V. M. Canário and J. Fuentes (2013). "Adaptation to different salinities exposes functional specialization in the intestine of the sea bream (*Sparus aurata* L.)." The Journal of Experimental Biology **216**(3): 470-479.
Grosell, M. (2011). "Intestinal anion exchange in marine teleosts is involved in osmoregulation and contributes to the oceanic inorganic carbon cycle." Acta Physiol (Oxf) **202**(3): 421-434.
Handeland, S. O., Björnsson, A. M. Arnesen and S. O. Stefansson (2003). "Seawater adaptation and growth of post-smolt Atlantic salmon (Salmo salar) of wild and farmed strains." Aquaculture **220**(1): 367-384.
Hoar, W. S. (1976). "Smolt Transformation: Evolution, Behavior, and Physiology." Journal of the Fisheries Research Board of Canada **33**(5): 1233-1252.
Hoar, W. S. (1988). 4 The Physiology of Smolting Salmonids. Fish Physiology. W. S. Hoar and D. J. Randall, Academic Press. **11:** 275-343.
Iversen, M., T. Mulugeta, B. Gellein Blikeng, A. C. West, E. H. Jørgensen, S. Rød Sandven and D. Hazlerigg (2020). "RNA profiling identifies novel, photoperiod-history dependent markers associated with enhanced saltwater performance in juvenile Atlantic salmon." PLOS ONE **15**(4): e0227496.
Khojasteh, S. M. B. (2012). "The morphology of the post-gastric alimentary canal in teleost fishes: a brief review." Int. J. of Aquatic Science **3**(2): 71-88.

Lebovitz, R. M., K. Takeyasu and D. M. Fambrough (1989). "Molecular characterization and expression of the (Na+ + K+)-ATPase alpha-subunit in Drosophila melanogaster." The EMBO Journal **8**(1): 193-202.
Lokka, G., L. Austbo, K. Falk, I. Bjerkas and E. O. Koppang (2013). "Intestinal morphology of the wild Atlantic salmon (Salmo salar)." J Morphol **274**(8): 859-876.
Loretz, C. A. (1995). 2 Electrophysiology of Ion Transport in Teleost Intestinal Cells. Fish Physiology. C. M. Wood and T. J. Shuttleworth, Academic Press. **14:** 25-56.
Lytle, C., J. C. Xu, D. Biemesderfer and B. Forbush, 3rd (1995). "Distribution and diversity of Na-K-Cl cotransport proteins: a study with monoclonal antibodies." Am J Physiol **269**(6 Pt 1): C1496-1505.
Marshall, W. S. (2002). "Na+, Cl−, Ca2+ and Zn2+ transport by fish gills: retrospective review and prospective synthesis." Journal of Experimental Zoology **293**(3): 264-283.
McCormick, S. and R. Saunders (1987). Preparatory Physiological Adaptations for Marine Life of Salmonids: Osmoregulation, Growth, and Metabolism.
McCormick, S. D. (2012). Smolt Physiology and Endocrinology. Euryhaline Fishes**:** 199-251.
McCormick, S. D., A. M. Regish and A. K. Christensen (2009). "Distinct freshwater and seawater isoforms of Na+/K+-ATPase in gill chloride cells of Atlantic salmon." J Exp Biol **212**(Pt 24): 3994-4001.
McCormick, S. D., J. M. Shrimpton, S. Moriyama and B. T. Björnsson (2007). "Differential hormonal responses of Atlantic salmon parr and smolt to increased daylength: A possible developmental basis for smolting." Aquaculture **273**(2): 337-344.
Musch, M. W., S. A. Orellana, L. S. Kimberg, M. Field, D. R. Halm, E. J. Krasny, Jr. and R. A. Frizzell (1982). "Na+-K+-Cl- co-transport in the intestine of a marine teleost." Nature **300**(5890): 351-353.
Nisembaum, L. G., P. Martin, F. Lecomte and J. Falcón (2021). "Melatonin and osmoregulation in fish: A focus on Atlantic salmon Salmo salar smoltification." J Neuroendocrinol **33**(3): e12955.
Parasram, K., N. Bernardon, M. Hammoud, H. Chang, L. He, N. Perrimon and P. Karpowicz (2018). "Intestinal Stem Cells Exhibit Conditional Circadian Clock Function." Stem Cell Reports **11**(5): 1287-1301.
Parasram, K. and P. Karpowicz (2020). "Time after time: circadian clock regulation of intestinal stem cells." Cellular and Molecular Life Sciences **77**(7): 1267-1288.
Peyric, E., H. A. Moore and D. Whitmore (2013). "Circadian Clock Regulation of the Cell Cycle in the Zebrafish Intestine." PLOS ONE **8**(8): e73209.
Preibisch, S., S. Saalfeld and P. Tomancak (2009). "Globally optimal stitching of tiled 3D microscopic image acquisitions." Bioinformatics **25**(11): 1463-1465.
Salman, N. A. (2009). "Effect of dietary salt on feeding, digestion, growth and osmoregulation in teleost fish." Essential reviews in experimental biology **1**: 109-150.
Salman, N. A. and F. B. Eddy (1987). "Response of chloride cell numbers and gill Na+K+ ATPase activity of freshwater rainbow trout (Salmo gairdneri Richardson) to salt feeding." Aquaculture **61**(1): 41-48.

Salman, N. A. and F. B. Eddy (1988). "Effect of dietary sodium chloride on growth, food intake and conversion efficiency in rainbow trout (Salmo gairdneri Richardson)." Aquaculture **70**(1): 131-144.
Schindelin, J., I. Arganda-Carreras, E. Frise, V. Kaynig, M. Longair, T. Pietzsch, S. Preibisch, C. Rueden, S. Saalfeld, B. Schmid, J. Y. Tinevez, D. J. White, V. Hartenstein, K. Eliceiri, P. Tomancak and A. Cardona (2012). "Fiji: an open-source platform for biological-image analysis." Nat Methods **9**(7): 676-682.
Stokes, K., A. Cooke, H. Chang, D. R. Weaver, D. T. Breault and P. Karpowicz (2017). "The Circadian Clock Gene BMAL1 Coordinates Intestinal Regeneration." Cellular and Molecular Gastroenterology and Hepatology **4**(1): 95-114.
Striberny, A., D. E. Lauritzen, J. Fuentes, M. A. Campinho, P. Gaetano, V. Duarte, D. G. Hazlerigg and E. H. Jørgensen (2021). "More than one way to smoltify a salmon? Effects of dietary and light treatment on smolt development and seawater growth performance in Atlantic salmon." Aquaculture **532**: 736044.
Sundell, K., F. Jutfelt, T. Ágústsson, R.-E. Olsen, E. Sandblom, T. Hansen and B. T. Björnsson (2003). "Intestinal transport mechanisms and plasma cortisol levels during normal and out-of-season parr–smolt transformation of Atlantic salmon, Salmo salar." Aquaculture **222**(1-4): 265-285.
Sundell, K. S. and H. Sundh (2012). "Intestinal fluid absorption in anadromous salmonids: importance of tight junctions and aquaporins." Front Physiol **3**: 388.
Sundh, H., T. O. Nilsen, J. Lindstrom, L. Hasselberg-Frank, S. O. Stefansson, S. D. McCormick and K. Sundell (2014). "Development of intestinal ion-transporting mechanisms during smoltification and seawater acclimation in Atlantic salmon Salmo salar." J Fish Biol **85**(4): 1227-1252.
Tipsmark, C., S. Madsen, M. Seidelin, A. Christensen, C. Cutler and G. Cramb (2002). "Dynamics of Na, K, 2C1 cotransporter and Na, K-ATPase expression in the branchial epithelium of brown trout (Salmo trutta) and Atlantic salmon (Salmo salar." The Journal of experimental zoology **293**: 106-118.
Veillette, P. A., R. J. White and J. L. Specker (1993). "Changes in intestinal fluid transport in Atlantic salmon (Salmo salar L) during parr-smolt transformation." Fish Physiol Biochem **12**(3): 193-202.
Zaugg, W. S. and L. R. McLain (1976). "Influence of water temperature on gill sodium, potassium-stimulated ATPase activity in juvenile coho salmon (Oncorhynchus kisutch)." Comparative Biochemistry and Physiology Part A: Physiology **54**(4): 419-421.

962 **Tables**

963 **Table 1:** Diet composition.

Diet composition	Control (%)	Salt (%)
Wheat	15.00	9.90
Wheat gluten	10.00	12.00
Sunflower meal	5.00	2.00
Soy protein concentrate	15.50	15.00
Fababean dehulled	4.80	2.00
Fish meal	31.30	32.30
Rapeseed oil	8.50	8.60
Fish oil	8.50	8.60
Water	0.30	1.00
Vitamin and mineral premixes	1.10	1.10
Sodium chloride	0.00	6.00
Calcium chloride	0.00	0.75
L-tryptophan	0.00	0.40
Magnesium chloride	0.00	0.25
Total	100.00	100.00
Moisture	8.30	8.30
Protein	43.55	43.24
Fat	21.99	21.99
Ash	6.98	13.36
Gross energy (MJ)	22.17	21.21

964

965

966

967

968

969

970

971

972

973

974

Figure Legends:

Figure 1 – Schematic of experimental design and sampling timeline of different treatments of Atlantic salmon. Light grey box and circles shows the treatments and samplings, respectively, on freshwater (FW). Dark grey box and circles corresponds to treatments and sampling on seawater (SW). Green line corresponds to the "control" group (treatment 1), maintained in continuously light during all the experiment. The orange line corresponds to treatment 2, the group of fishes will be given feed enriched with salt and amino-acid mix for 6 weeks ("diet" group). Treatment 3 receives a light regime of 7h light/17h dark for 6 weeks ("light" group) and is represented by blue line. Treatment 4, red line, is a combination of light and diet treatments ("light & diet" group). Before the first sampling on FW, the fish were maintained at constant light and 10ºC. The second and the third samplings will be after 6 weeks of light and diet treatments, respectively. Sampling after 1 day in SW corresponds to circle SW1, and sampling SW7 and SW60 corresponds at 7 days and 60 days after SW transfer, respectively.

Figure 2 – Morphometric measurements in intestine of Atlantic salmon. A – D: morphometric measurements in anterior intestine. **E – H:** morphometric measurements in posterior intestine. A and E: Ratio of the external perimeter (P_{ext}) over the total length of the fish (P_{ext}/TL_{mean}). B and F: Ratio between absorptive surface perimeter and external perimeter (Pabs/Pext). C and G: Ratio between *villi* and external perimeter (*villi*/P_{ext}). D and H: Ratio between the wall thickness and external perimeter of the intestine (Thickness/P_{ext}). The ratios were calculated to the beginning of the experiment (FW1), after light regime (FW2), after dietary treatment and before SW transfer (FW3), 1 day after SW transfer (SW1), 7 days after SW transfer (SW7) and after 60 days SW transfer (SW60), and it were represented in a box-and-whisker diagram. Each box represents the 25^{th} and 75^{th} percentiles, the line in the middle of the box indicated the median and whiskers represent the highest and lowest values (n=2-5). In the analysis, light and dietary treatment are the considered factors; different uppercase capital letters indicate significant differences among experimental groups in each time point; significant p values are reported in the graph ($p<0.05$, two-way ANOVA,

followed by Bonferroni post-hoc test). Small letters on FW2 indicates significant differences between LL-LL and SP-LL groups ($p<0.05$, unpaired t-student test).

Figure 3 – Cell proliferation percentage in intestine of Atlantic salmon undergoing smoltification and SW adaptation. A: Percentage of cell proliferation in anterior intestine. **B:** Percentage of cell proliferation in posterior intestine. The ratio between cells marked with PCNA and total number of cells in a villus was calculated to the first sampling in FW (FW1), after light regime (FW2), after dietary treatment and before SW transfer (FW3), 1 day after SW transfer (SW1), 7 days after SW transfer (SW7) and after 60 days SW transfer (SW60), and it were represented in a box-and-whisker diagram. Each box represents the 25^{th} and 75^{th} percentiles, the line in the middle of the box indicated the median and whiskers represent the highest and lowest values (number of fish=2-5). In the analysis, light and dietary treatment are the considered factors; different uppercase capital letters indicate significant differences among experimental groups in each time point; significant p values are reported in the graph ($p<0.05$, two-way ANOVA, followed by Bonferroni post-hoc test). Small letters on Mar FW indicates significant differences between LL-LL and SP-LL groups ($p<0.05$, unpaired t-student test).

Figure 4 – Na+ K+ -ATPase total intensity in anterior and posterior intestines of Atlantic salmon. A: Ratio between total intensity and the total number of nucleus of anterior intestine. **B:** Ratio between total intensity and the total number of nucleus of posterior intestine. The first sampling in FW (FW1), after light regime (FW2), after dietary treatment and before SW transfer (FW3), 1 day after SW transfer (SW1), 7 days after SW transfer (SW7) and after 60 days SW transfer (SW60), were represented in a box-and-whisker diagram in axis X. Each box represents the 25^{th} and 75^{th} percentiles, the line in the middle of the box indicated the median and whiskers represent the highest and lowest values (number of fish=2-5). In the analysis, light and dietary treatment are the considered factors; different uppercase capital letters indicate significant differences among experimental groups in each time point; significant p values are reported in the graph ($p<0.05$, two-way ANOVA, followed by Bonferroni post-hoc

test). Small letters on Mar FW indicates significant differences between LL-LL and SP-LL groups ($p<0.05$, unpaired t-student test).

Figure 5 – Na+ K+ 2Cl- co transporter (NKCC) total intensity and distribution on anterior and posterior intestines of Atlantic salmon. A: Ratio between total intensity of NKCC and the total number of nucleus in a villus of anterior intestine. **B:** Ratio between total intensity of NKCC and the total number of nucleus in a villus of posterior intestine. The first sampling in FW ((FW1), after light regime (FW2), after dietary treatment and before SW transfer (FW3), 1 day after SW transfer (SW1), 7 days after SW transfer (SW7) and after 60 days SW transfer (SW60), were represented in a box-and-whisker diagram in axis X. Each box represents the 25^{th} and 75^{th} percentiles, the line in the middle of the box indicated the median and whiskers represent the highest and lowest values (number of fish=2-5). In the analysis, light and dietary treatment are the considered factors; different uppercase capital letters indicate significant differences among experimental groups in each time point; significant p values are reported in the graph ($p<0.05$, two-way ANOVA, followed by Bonferroni post-hoc test). Small letters on Mar FW indicate significant differences between LL-LL and SP-LL groups ($p<0.05$, unpaired t-student test).

Figure 1

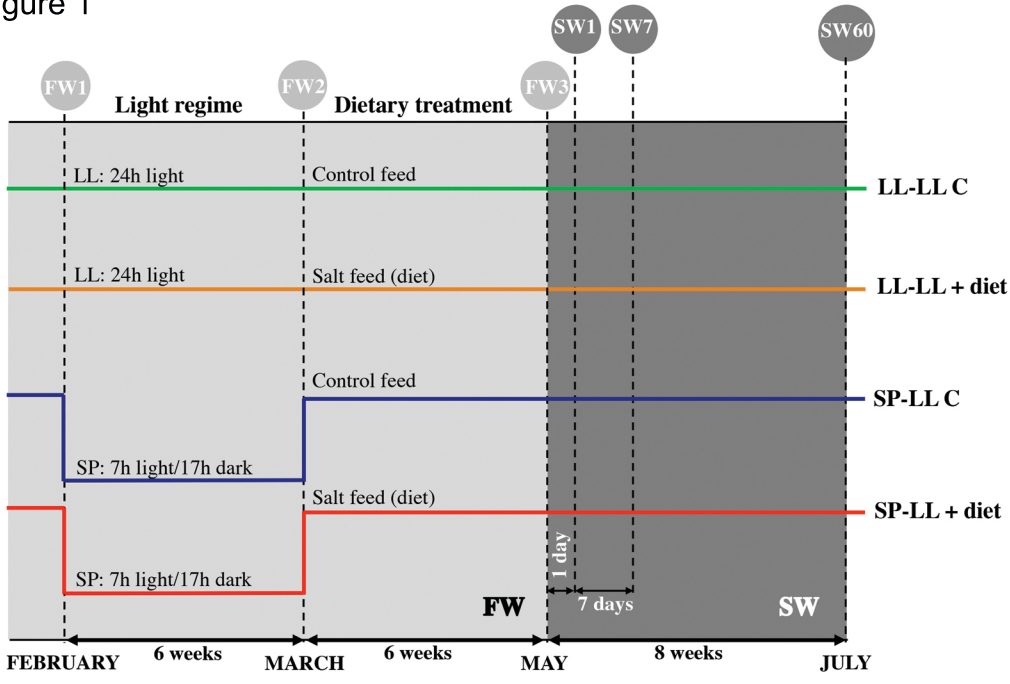
SW1
SW7
SW60
FW1
FW2
FW3
Light regime
Dietary treatment
LL: 24h light
Control feed
LL-LL C
LL: 24h light
Salt feed (diet)
LL-LL + diet
Control feed
SP-LL C
SP: 7h light/17h dark
Salt feed (diet)
SP-LL + diet
SP: 7h light/17h dark
1 day
7 days
FW
SW
FEBRUARY
6 weeks
MARCH
6 weeks
MAY
8 weeks
JULY

Figure 2

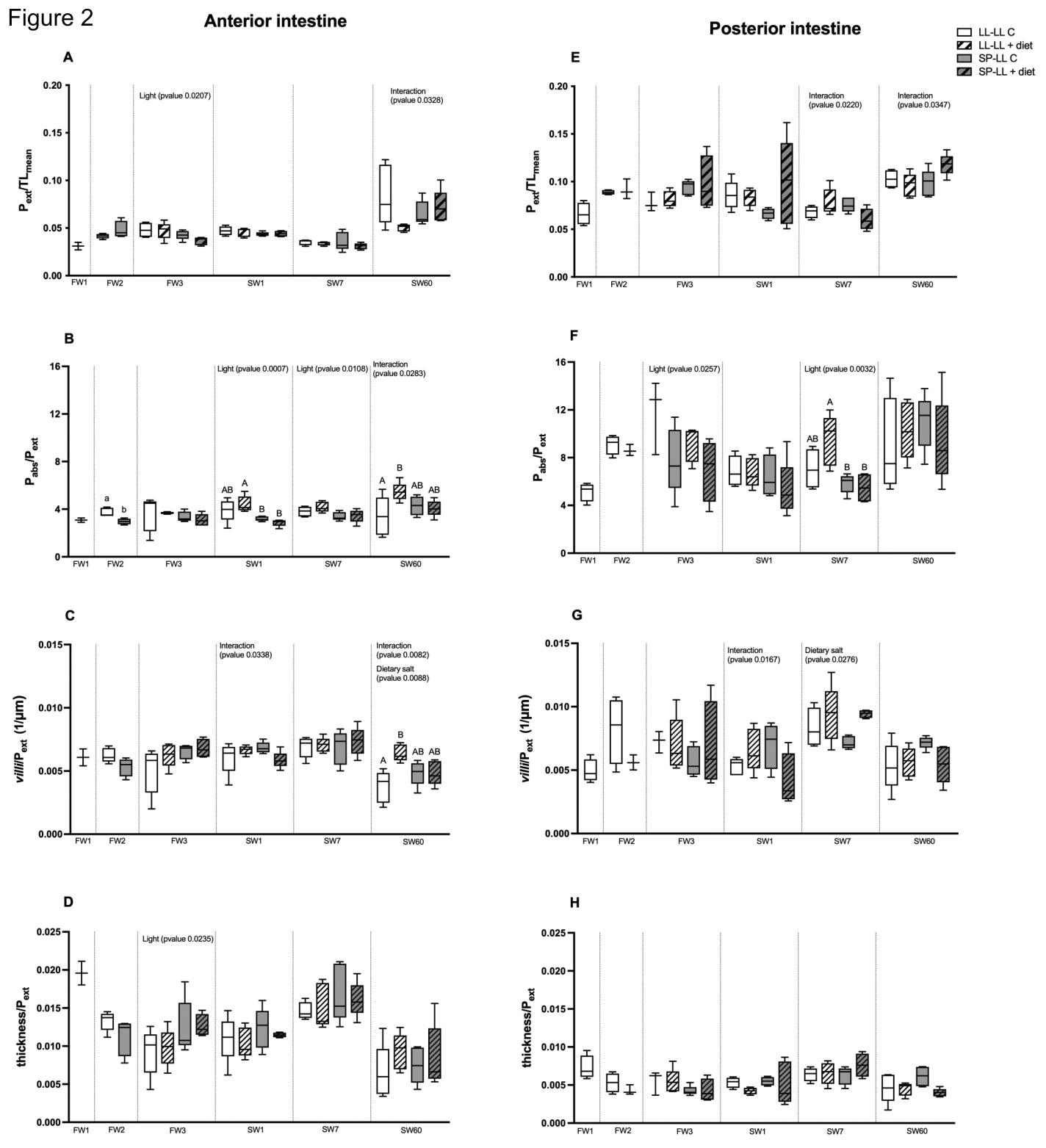
Anterior intestine
Posterior intestine
LL-LL C
LL-LL + diet
SP-LL C
SP-LL + diet
A
B
C
D
E
F
G
H
P_{ext}/TL_{mean}
P_{abs}/P_{ext}
villi//P_{ext} (1/µm)
thickness/P_{ext}
FW1
FW2
FW3
SW1
SW7
SW60
Light (pvalue 0.0207)
Interaction (pvalue 0.0328)
Light (pvalue 0.0007)
Light (pvalue 0.0108)
Interaction (pvalue 0.0283)
Interaction (pvalue 0.0338)
Interaction (pvalue 0.0082)
Dietary salt (pvalue 0.0088)
Light (pvalue 0.0235)
Interaction (pvalue 0.0220)
Interaction (pvalue 0.0347)
Light (pvalue 0.0257)
Light (pvalue 0.0032)
Interaction (pvalue 0.0167)
Dietary salt (pvalue 0.0276)

Figure 3

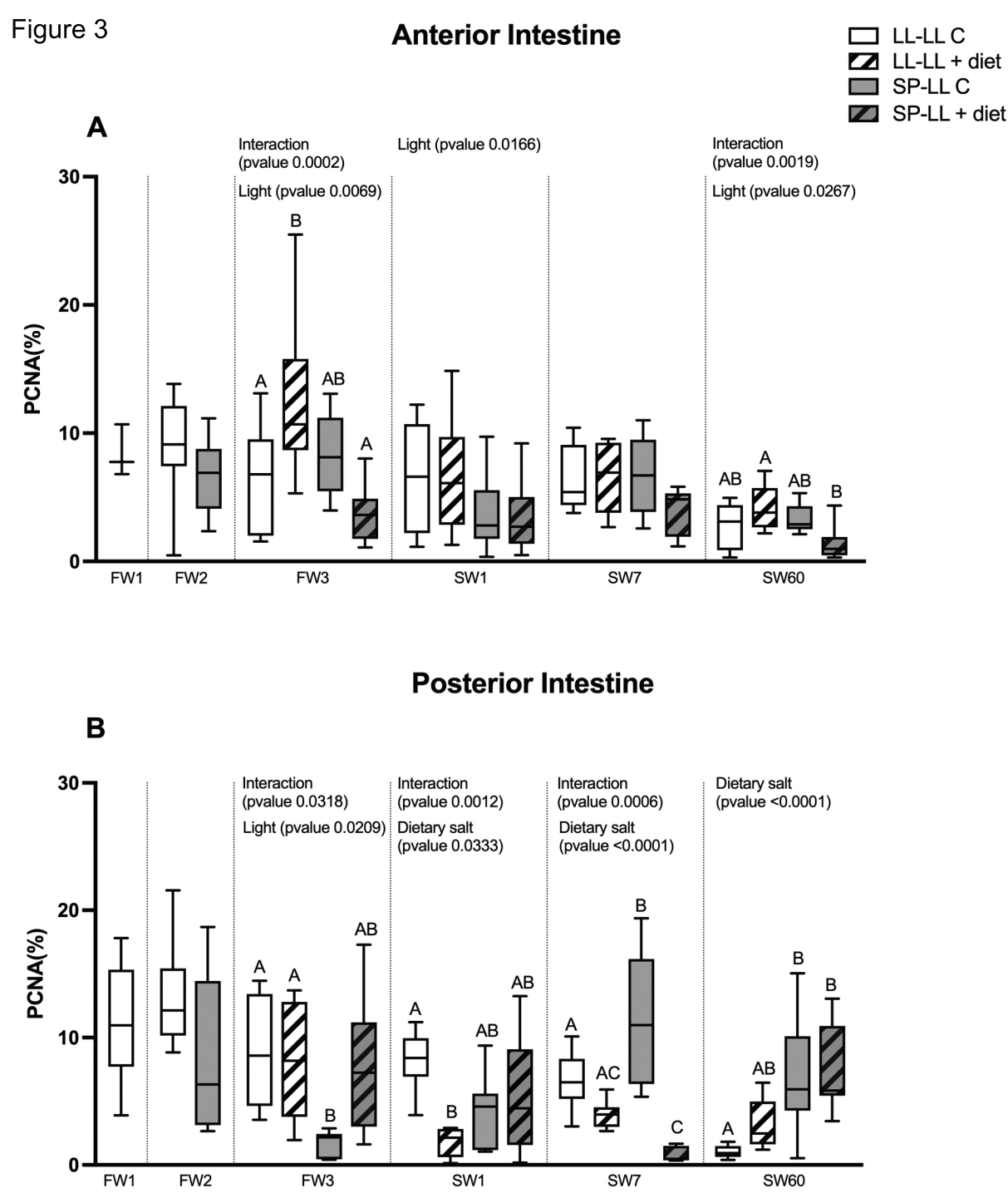
Anterior Intestine
LL-LL C
LL-LL + diet
SP-LL C
SP-LL + diet
A
Interaction (pvalue 0.0002)
Light (pvalue 0.0069)
Light (pvalue 0.0166)
Interaction (pvalue 0.0019)
Light (pvalue 0.0267)
PCNA(%)
30
20
10
0
A
B
AB
A
AB
A
AB
B
FW1
FW2
FW3
SW1
SW7
SW60
Posterior Intestine
B
Interaction (pvalue 0.0318)
Light (pvalue 0.0209)
Interaction (pvalue 0.0012)
Dietary salt (pvalue 0.0333)
Interaction (pvalue 0.0006)
Dietary salt (pvalue <0.0001)
Dietary salt (pvalue <0.0001)
PCNA(%)
30
20
10
0
A
A
B
AB
A
B
AB
AB
A
AC
B
C
A
AB
B
B
FW1
FW2
FW3
SW1
SW7
SW60

Figure 4

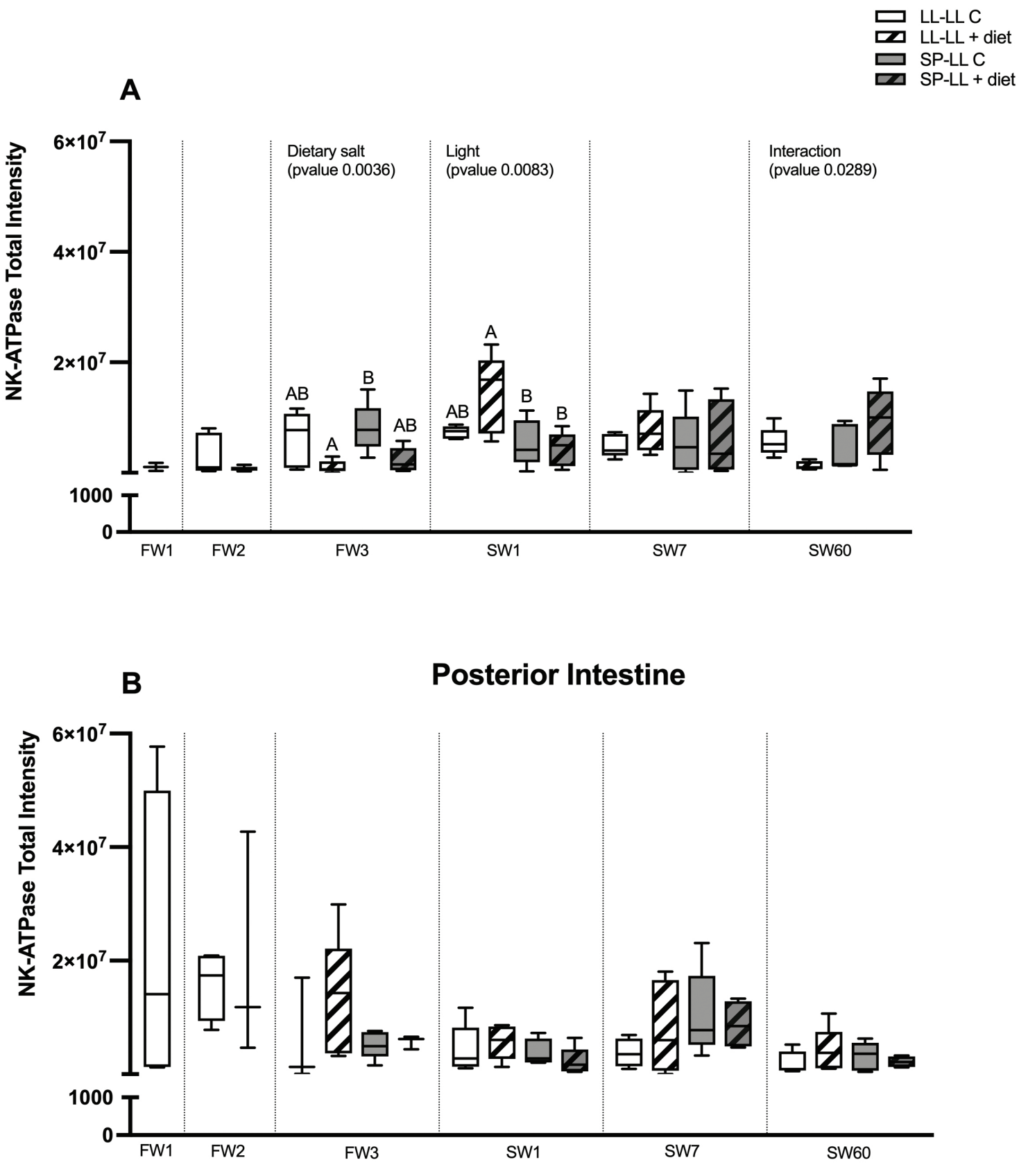
Anterior Intestine
LL-LL C
LL-LL + diet
SP-LL C
SP-LL + diet
A
NK-ATPase Total Intensity
6×10^7
4×10^7
2×10^7
1000
0
Dietary salt
(pvalue 0.0036)
Light
(pvalue 0.0083)
Interaction
(pvalue 0.0289)
AB
A
B
AB
AB
A
B
B
FW1
FW2
FW3
SW1
SW7
SW60
B
Posterior Intestine
NK-ATPase Total Intensity
6×10^7
4×10^7
2×10^7
1000
0
FW1
FW2
FW3
SW1
SW7
SW60

Figure 5

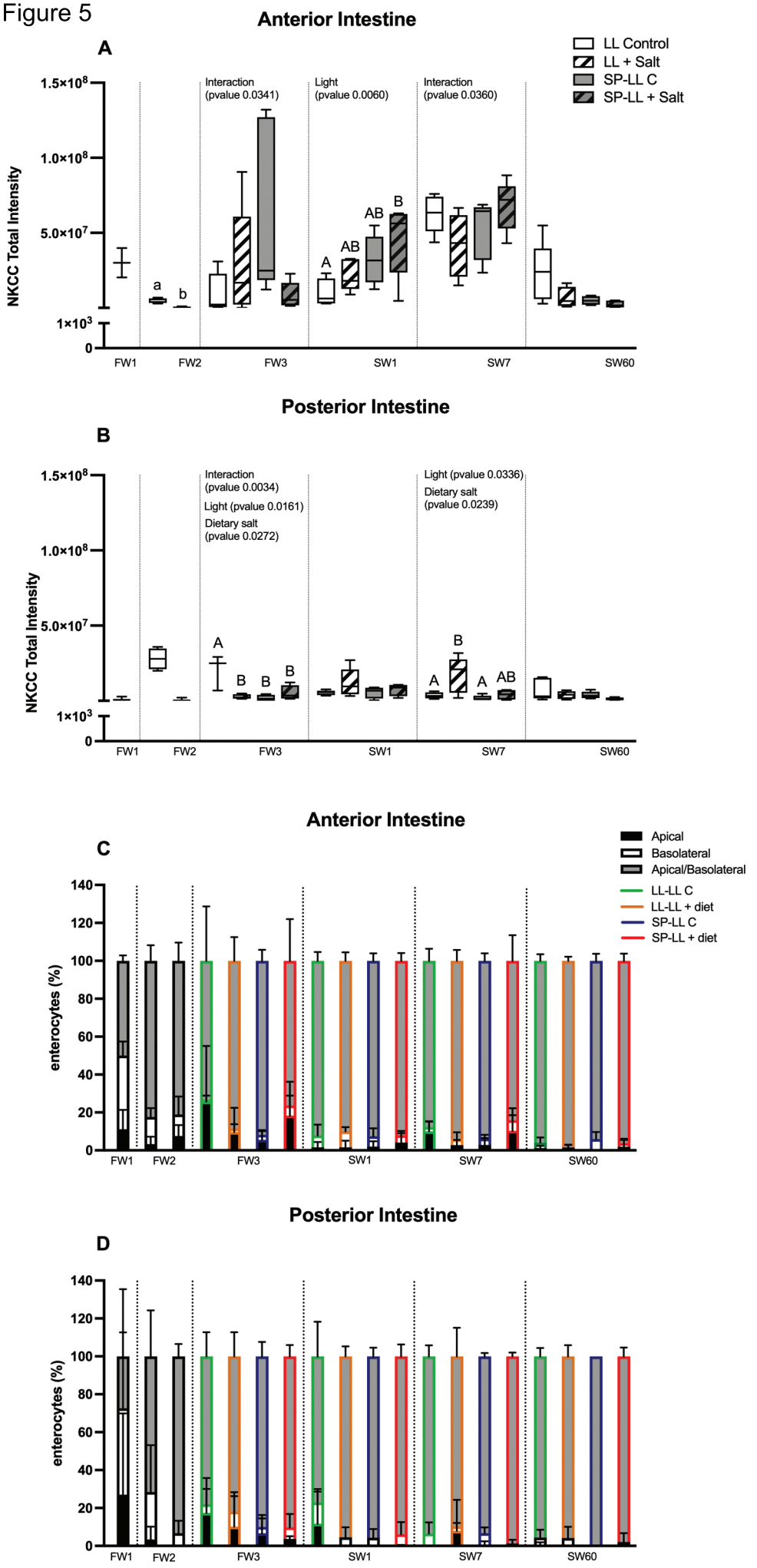
Anterior Intestine
A
LL Control
LL + Salt
SP-LL C
SP-LL + Salt
NKCC Total Intensity
1.5×10^8
1.0×10^8
5.0×10^7
1×10^3
0
Interaction (pvalue 0.0341)
Light (pvalue 0.0060)
Interaction (pvalue 0.0360)
a
b
A
AB
AB
B
FW1
FW2
FW3
SW1
SW7
SW60
Posterior Intestine
B
Interaction (pvalue 0.0034)
Light (pvalue 0.0161)
Dietary salt (pvalue 0.0272)
Light (pvalue 0.0336)
Dietary salt (pvalue 0.0239)
A
B
B
B
A
B
A
AB
Anterior Intestine
C
Apical
Basolateral
Apical/Basolateral
LL-LL C
LL-LL + diet
SP-LL C
SP-LL + diet
enterocytes (%)
140
120
100
80
60
40
20
0
FW1
FW2
FW3
SW1
SW7
SW60
Posterior Intestine
D
enterocytes (%)
140
120
100
80
60
40
20
0
FW1
FW2
FW3
SW1
SW7
SW60